DNA Photochemistry

DOI: 10.1002/anie.201008146

# Hydrogen Bonding Regulates the Monomeric Nonradiative Decay of Adenine in DNA Strands**

*You Lu, Zhenggang Lan,* and Walter Thiel**

It has been suggested in ultrafast spectroscopic studies that excited states localized on single nucleobases as well as delocalized exciton or excimer/exciplex states contribute towards the nonradiative decay of DNA helices.[1–11] Unlike the situation in the gas phase and in water, where the internal conversions through conical intersections (CIs) are reasonably well understood,[12,13] little is known about the decay mechanisms of single nucleobases in DNA. Experimentally, it is difficult to identify the different decay channels,[9] and the excited-state decay of DNA model systems is extremely complex, being wavelength dependent and showing multiexponential behavior, with time constants ranging from the sub-ps regime to 100 ps and beyond.[2–11,14,15] There are several recent computational studies on this topic,[1,16–26] but one central question is still unanswered: how is the mechanism of radiationless decay on an individual nuleobase affected by the biological environment of DNA?

Herein, we study the nonradiative decay dynamics of a single adenine embedded within solvated oligonucleotides by QM/MM[27,28] calculations. The dynamics were simulated in silico by on-the-fly surface-hopping calculations.[29,30] To mimic DNA single and double strands, two B-type oligomer models $(dA)_{10}$ and $(dA)_{10}\cdot(dT)_{10}$ were constructed by using Maestro 7.5.[31] They were solvated in spherical water droplets described by the TIP3P model.[32] The DNA charges were neutralized with $Na^+$ ions using SYBYL 8.0.[33] For either model, the QM region contained 14 atoms from an adenine located near the center of the system, while the MM region consisted of all remaining atoms.

After setting up the models, QM/MM simulations were carried out using a development version of the ChemShell package.[34–36] The QM subsystem (QM adenine) was treated by the OM2/MRCI approach[37–40] (semiempirical orthogonalization model 2 combined with multireference configuration interaction) using a (12,10) active space (12 electrons in 10 orbitals).[41,42] The MM part was handled by the DL_POLY package[43] applying the CHARMM27 force field.[44] Born–Oppenheimer molecular dynamics (BOMD) simulations at 300 K were performed for both oligonucleotides in their electronic ground state, for initial sampling and for computing electronic absorption spectra. Thereafter, surface-hopping simulations involving the three lowest adiabatic states ($S_0$, $S_1$, and $S_2$) were run up to 1.5 ps. Details of the computational procedures are given in the Supporting Information.

The choice of the computational model (a single QM adenine in an MM environment) restricts the present study to monomeric excitation and decay processes. Hence we do not consider excitons (delocalized over stacked bases)[2–5,11,16,17,45] or excimer/exciplex states,[6–13] nor do we treat electron- or proton-transfer processes among hydrogen-bonded nucleobases,[19,46–49] in spite of their important role in DNA. Another limitation is the use of a semiempirical QM/MM approach, which is dictated by the need for computational efficiency[36] and limits the accuracy that can be attained. OM2/MRCI has recently been applied successfully to study the excited-state dynamics of nucleobases,[41,42,50,51] and we refer the readers to the work on adenine in the gas phase[41] and in aqueous solution[42] for a detailed discussion of accuracy issues, including comparisons with high-level ab initio results for gas-phase adenine. On this basis the current QM/MM approach is expected to provide realistic results, especially with regard to the influence of the environment on the photophysics of adenine.

Figure 1 shows the Gaussian-broadened absorption bands relevant to the three lowest-lying excited states ($S_1$, $S_2$, and $S_3$) of adenine in $(dA)_{10}$ and $(dA)_{10}\cdot(dT)_{10}$. The $S_1$ state is found to be bright in the both helices. The absorption maximum occurs at 4.71 eV for adenine in $(dA)_{10}$, somewhat lower than the experimental value[20] of 4.82 eV for $(dA)_{20}$. Analogous results are found for $(dA)_{10}\cdot(dT)_{10}$ whose calculated absorption maximum is at 4.78 eV, again close to or slightly lower than the experimental values of 4.78 eV for $(dA)_{20}\cdot(dT)_{20}$ and

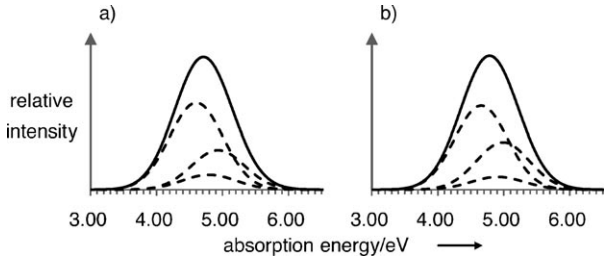


***Figure 1.*** Absorption spectrum calculated by the QM/MM (QM = OM2/MRCI) approach for 200 snapshots from ground-state BOMD simulations (with Gaussian broadening). a) $(dA)_{10}$, maximum at 4.71 eV; b) $(dA)_{10}\cdot(dT)_{10}$, maximum at 4.78 eV. The overall bands (solid) can be decomposed into contributions from the three lowest-energy transitions (shown as dashed lines).

[*] Y. Lu, Dr. Z. Lan, Prof. Dr. W. Thiel
Max-Planck-Institut für Kohlenforschung
Kaiser-Wilhelm-Platz 1, 45470 Mülheim an der Ruhr (Germany)
Fax: (+49) 208-306-2996
E-mail: lan@mpi-muelheim.mpg.de
thiel@mpi-muelheim.mpg.de

[**] We are grateful to Dr. Mario Barbatti and Dr. Eduardo Fabiano for valuable discussions and to Dr. Tell Tuttle for his help in setting up the QM/MM calculations.

Supporting information for this article is available on the WWW under http://dx.doi.org/10.1002/anie.201008146.

4.84 eV for $(dA)_n \cdot (dT)_n$.[17,45] The current QM/MM computations thus tend to underestimate the first absorption maximum in DNA strands by up to 0.11 eV, in analogy to the situation in the gas phase (0.19 eV) and in aqueous solution (0.10 eV).[41,42] We note in this context that Frenkel excitons (not covered presently) should cause a blue shift of the absorption compared with the monomers.[1,16,17,21,45]

During the initial BOMD ground-state sampling, the $S_1$ and $S_2$ states are populated according to their oscillator strengths. This leads to a minority of trajectories [12% for adenine in $(dA)_{10}$ and 19% in $(dA)_{10} \cdot (dT)_{10}$] that start from the $S_2$ state. For these trajectories, the $S_2 \rightarrow S_1$ decay takes place extremely rapidly (mean lifetime ca. 7 fs, see Figure 2),

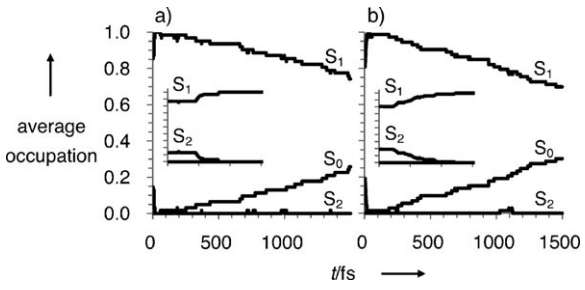


***Figure 2.*** Average occupations of adenine. a) $(dA)_{10}$, 64 trajectories starting from $S_1$ and 9 from $S_2$; b) $(dA)_{10} \cdot (dT)_{10}$, 59 trajectories starting from $S_1$ and 14 from $S_2$. Dynamics within the initial 30 fs are shown in the insets.

distinctly faster than in the gas phase or in water.[41,42] Thereafter, the $S_1$ state undergoes nonradiative decay through the $S_0/S_1$ CIs on the timescale of several picoseconds. Exponential fitting gives mean $S_1$ lifetimes of 5.7 ps and 4.1 ps for adenine in $(dA)_{10}$ and $(dA)_{10} \cdot (dT)_{10}$, respectively.

Compared with the results in the gas phase and in water,[41,42] the decay dynamics of an individual adenine is thus slowed down (by an order of magnitude) when it is embedded in DNA helices. Several factors are responsible for this deceleration. First, the biological environment in DNA lowers the interstate coupling and thus reduces the electronic hopping probability (see the Supporting Information). Second, the $S_0/S_1$ CIs are generally characterized by strong out-of-plane distortions (see below), and the motion towards such a CI is impeded for steric reasons since it brings the bending atom or functional group close to the adjacent nucleobase. Finally, there is another $S_1$ minimum of adenine close to the dominant $S_0/S_1$ CI, which is more pronounced in DNA than in the gas phase and may thus further delay the hopping by acting as a trap for the trajectories (see the Supporting Information). Experimental studies[2–11,14,15] have reported time constants from multi-exponential fits of spectroscopic data in DNA base multimers that typically cluster in three ranges (0.2–0.6 ps, 2–6 ps, and 100–200 ps), which have been associated with monomeric internal conversion,[2–11] vibrational cooling[6,11] or exciton/excimer processes,[7–11] and the decay of delocalized states,[2–11,15] respectively. The current calculations indicate monomeric decay in the low ps range. This suggests that in this range monomeric nonradiative processes may also contribute to the experimentally observed decay in DNA strands,[2–11,14,15] without ruling out other decay channels in the complex electrostatic and steric environment of DNA.[6,7,52–54]

In spite of the fact that the computed time constants for the $S_1 \rightarrow S_0$ nonradiative decay of adenine are similar in DNA single and double strands, the decay channels are found to be quite different. Considering the $(dA)_{10}$ single strand first, 19 of a total of 73 trajectories (26%) hop to the $S_0$ surface within 1.5 ps. In 11 of these, the dihedral angle $|\measuredangle(N_1C_5C_6N_6)|$ (Figure 3d) is less than 145° at the $S_1 \rightarrow S_0$ hopping events

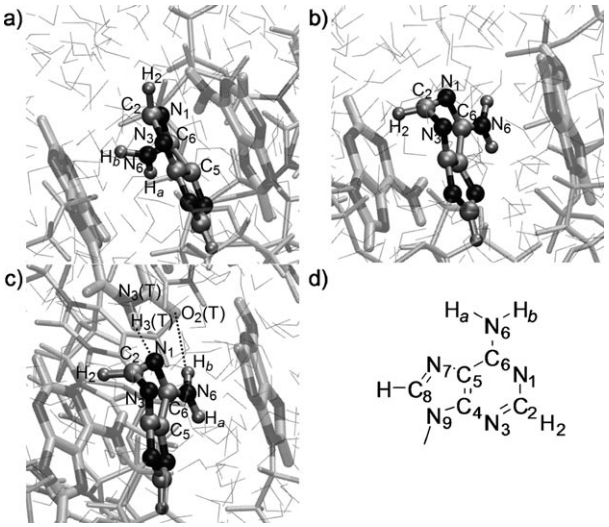


***Figure 3.*** Typical structures at conical intersections of adenine: a) $^6S_1$ channel in $(dA)_{10}$; b) $^2E$ channel in $(dA)_{10}$; c) $^2E$ channel in $(dA)_{10} \cdot (dT)_{10}$; d) chemical structure of adenine. In these VMD[66] pictures, the QM adenines are drawn as ball-and-stick representations, and the adjacent bases are drawn as bold-licorice representations. The A–T hydrogen bonds are highlighted in (c).

(Figure 4a), indicating a decay via the $S_0/S_1$ CI that is characterized by an out-of-plane deformation of the amino group and a ring puckering at the $C_6$ atom (Figure 3a).[55–58] According to the Cremer–Pople–Boeyens classification,[59,60]

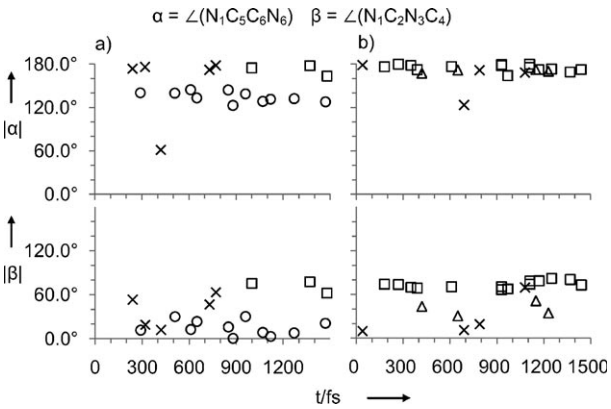


***Figure 4.*** Scatter plots of some key geometric parameters at the $S_1 \rightarrow S_0$ hopping events for adenine in: a) $(dA)_{10}$ and b) $(dA)_{10} \cdot (dT)_{10}$. Hops occur via the $^6S_1$ channel (○), the $^2E$ channel (□), the screw-boat channel (△), and side reactions (×), see text for details.

  

this type of CI has been assigned[58] as $^6S_1$ for adenine in the gas phase (see the Supporting Information for details). In three trajectories, the nonradiative decay occurs via the $S_0/^1L_a$ CI that is identified by the puckering of the six-membered ring at the $C_2$ atom and the bending of the $H_2$ atom (see Figure 3b and Figure 4a)[55–58] and is labeled[58] as the $^2E$ channel. The remaining five trajectories follow diverse pathways before $S_1 \rightarrow S_0$ hopping events, including ring decomposition and $C_2$–$H_2$ or $C_8$–$H_8$ cleavage, which may be considered as side reactions. For adenine in $(dA)_{10}$, the $^6S_1$ channel thus represents the primary monomer pathway for returning to the ground state.

Turning to adenine in the $(dA)_{10}\cdot(dT)_{10}$ double strand, 22 of 73 trajectories (29%) show $S_1 \rightarrow S_0$ nonradiative decay within 1.5 ps. The majority of these (14) proceed via the $^2E$ CI by means of $C_2$-puckering and $H_2$-bending (see Figure 3c), with dihedral angles $|\measuredangle(N_1C_2N_3C_4)|$ of typically 60–80° at the hops (see Figure 3d and Figure 4b), exactly as for the $^2E$ channel in $(dA)_{10}$. Four trajectories hop to $S_0$ when the molecular plane folds along the $C_4$–$C_5$ axis and the six-membered ring puckers at $N_3$ to yield a screw-boat structure, similar to the $^4S_3$ conformation reported in reference [58] (see Figure 4b and the Supporting Information). The remaining four trajectories return to the ground state through side reactions such as the breaking of the five-membered ring, H-migration from $C_2$ to $N_3$, or $C_8$–$H_8$ cleavage. Most notably, no trajectory of adenine in $(dA)_{10}\cdot(dT)_{10}$ decays to $S_0$ by the $^6S_1$ mechanism.

Our previous studies at the same semiempirical OM2/MRCI level have shown that the $^6S_1$ CI plays a dominant role in the nonradiative decay of adenine in vacuo and in water,[41,42] where more than 90% of the trajectories pass the $^6S_1$ CI and only less than 10% decay via the $^2E$ channel. When adenine is surrounded by single-strand DNA in water, the $^6S_1$ channel is still dominant (ca. 60%), even though the $^2E$ channel and others become more important. For adenine in duplex DNA, two hydrogen bonds, $N_6H^A\cdots O_2{}^T$ and $N_1{}^A\cdots H_3{}^T$, are formed in each Watson–Crick adenine–thymine base pair (see Figure 3c). Since the amino group of adenine is involved in the first hydrogen bond, its out-of-plane motion will be restrained. In all 22 trajectories that show a nonadiabatic transition, the $N_6H^A\cdots O_2{}^T$ hydrogen bond is retained, with $N_6H^A\cdots O_2{}^T$ distances ranging between 2.8 and 3.6 Å during the 1.5 ps simulation time (see the Supporting Information); the corresponding value in the crystal structure is 2.80 Å.[61] In the nonradiative decay of adenine in $(dA)_{10}\cdot(dT)_{10}$, the $^6S_1$ channel is thus completely suppressed, and the $^2E$ channel becomes dominant. This clearly demonstrates that the mechanism for the internal conversion of adenine to the electronic ground state is controlled by the biological environment.

Generally speaking, the results from excited-state dynamics are largely governed by the topology of the underlying potential energy surfaces. In adenine, there is not yet consensus on some of these features among different theoretical approaches.[42] For example, in the gas phase, the path to the $^6S_1$ CI is essentially barrierless in some studies,[41,58,62] but not in others,[56,63,64] which will clearly affect the dynamical preferences. Hence, the outcome of dynamics studies should be viewed with caution and in the context of other theoretical work. Based on ab initio QM/MM reaction path calculations, Conti et al.[25] propose the $^2E$ channel as the leading pathway for the nonradiative decay of adenine in $(dA)_{10}\cdot(dT)_{10}$ (in accord with the present work), but they also favor this channel in the gas phase (as opposed to the $^6S_1$ channel in OM2/MRCI[41]). A recent ab initio QM/MM dynamics study[65] on a stacked trimer model (4-aminopyrimidine between two methyl guanine molecules) reports analogous decay mechanisms in isolated and stacked 4-aminopyrimidine (via similarly distorted CIs), a slight increase in the lifetime, and a notable dynamical influence of hydrogen bonding; such features are also apparent in our present work.

To summarize, we performed QM/MM surface-hopping simulations to investigate the nonradiative decay dynamics of adenine embedded within solvated DNA strands. For an individual adenine unit in $(dA)_{10}$ and $(dA)_{10}\cdot(dT)_{10}$, the time constants for internal conversion to the electronic ground state were computed to be 5.7 ps and 4.1 ps, respectively. They are about ten times longer than in vacuo or in water. Our simulations indicate that the $^6S_1$ ($C_6$-puckering and amino-bending) channel plays a leading role in the nonradiative decay of a single adenine in $(dA)_{10}$, while the $^2E$ ($C_2$-puckering and $H_2$-bending) channel coexists. By contrast, for adenine in $(dA)_{10}\cdot(dT)_{10}$, the $^6S_1$ mechanism is completely suppressed by hydrogen bonding between adenine and thymine, and the $^2E$ channel becomes dominant. We regard this surface-hopping study on an individual adenine unit in a realistic environment of nucleotides as an initial step towards more complete simulations of the complex excited-state dynamics in DNA. Being reasonably efficient and realistic, the current QM/MM (QM = OM2/MRCI) approach should be a useful tool for such theoretical investigations into DNA photochemistry.

Received: December 23, 2010
Revised: May 12, 2011
Published online: June 9, 2011

**Keywords:** DNA · hydrogen bonds · molecular dynamics · photochemistry · semiempirical calculations

[1] E. Emanuele, K. Zakrzewska, D. Markovitsi, R. Lavery, P. Millié, *J. Phys. Chem. B* **2005**, *109*, 16109–16118.
[2] D. Onidas, T. Gustavsson, E. Lazzarotto, D. Markovitsi, *J. Phys. Chem. B* **2007**, *111*, 9644–9650.
[3] D. Onidas, T. Gustavsson, E. Lazzarotto, D. Markovitsi, *Phys. Chem. Chem. Phys.* **2007**, *9*, 5143–5148.
[4] D. Markovitsi, T. Gustavsson, F. Talbot, *Photochem. Photobiol. Sci.* **2007**, *6*, 717–724.
[5] D. Markovitsi, T. Gustavsson, I. Vayá, *J. Phys. Chem. Lett.* **2010**, *1*, 3271–3276.
[6] T. Takaya, C. Su, K. de La Harpe, C. E. Crespo-Hernández, B. Kohler, *Proc. Natl. Acad. Sci. USA* **2008**, *105*, 10285–10290.
[7] C. T. Middleton, K. de La Harpe, C. Su, Y. K. Law, C. E. Crespo-Hernández, B. Kohler, *Annu. Rev. Phys. Chem.* **2009**, *60*, 217–239.
[8] C. E. Crespo-Hernández, B. Cohen, B. Kohler, *Nature* **2005**, *436*, 1141–1144.
[9] B. Kohler, *J. Phys. Chem. Lett.* **2010**, *1*, 2047–2053.

  

[10] W.-M. Kwok, C. Ma, D. L. Phillips, *J. Am. Chem. Soc.* **2006**, *128*, 11894 – 11905.
[11] I. Buchvarov, Q. Wang, M. Raytchev, A. Trifonov, T. Fiebig, *Proc. Natl. Acad. Sci. USA* **2007**, *104*, 4794 – 4797.
[12] C. E. Crespo-Hernández, B. Cohen, M. H. Patrick, B. Kohler, *Chem. Rev.* **2004**, *104*, 1977 – 2020.
[13] C. E. Crespo-Hernández, B. Kohler, *J. Phys. Chem. B* **2004**, *108*, 11182 – 11188.
[14] D. Markovitsi, A. Sharonov, D. Onidas, T. Gustavsson, *ChemPhysChem* **2003**, *4*, 303 – 305.
[15] N. Schwalb, F. Temps, *Science* **2008**, *322*, 243 – 245.
[16] B. Bouvier, T. Gustavsson, D. Markovitsi, P. Millié, *Chem. Phys.* **2002**, *275*, 75 – 92.
[17] B. Bouvier, J. P. Dognon, R. Lavery, D. Markovitsi, P. Millié, D. Onidas, K. Zakrzewska, *J. Phys. Chem. B* **2003**, *107*, 13512 – 13522.
[18] E. R. Bittner, *J. Chem. Phys.* **2006**, *125*, 094909.
[19] G. Groenhof, L. V. Schäfer, M. Boggio-Pasqua, M. Goette, H. Grubmüller, M. A. Robb, *J. Am. Chem. Soc.* **2007**, *129*, 6812 – 6819.
[20] L. Hu, Y. Zhao, F. Wang, G. Chen, C. Ma, W.-M. Kwok, D. L. Phillips, *J. Phys. Chem. B* **2007**, *111*, 11812 – 11816.
[21] R. Improta, *Phys. Chem. Chem. Phys.* **2008**, *10*, 2656 – 2664.
[22] S. Tonzani, G. C. Schatz, *J. Am. Chem. Soc.* **2008**, *130*, 7607 – 7612.
[23] A. W. Lange, J. M. Herbert, *J. Am. Chem. Soc.* **2009**, *131*, 3913 – 3922.
[24] E. B. Starikov, G. Cuniberti, S. Tanaka, *J. Phys. Chem. B* **2009**, *113*, 10428 – 10435.
[25] I. Conti, P. Altoè, M. Stenta, M. Garavelli, G. Orlandi, *Phys. Chem. Chem. Phys.* **2010**, *12*, 5016 – 5023.
[26] A. N. Alexandrova, J. C. Tully, G. Granucci, *J. Phys. Chem. B* **2010**, *114*, 12116 – 12128.
[27] H.-M. Senn, W. Thiel, *Top. Curr. Chem.* **2007**, *268*, 173 – 290.
[28] H.-M. Senn, W. Thiel, *Angew. Chem.* **2009**, *121*, 1220 – 1254; *Angew. Chem. Int. Ed.* **2009**, *48*, 1198 – 1229.
[29] J. C. Tully, *J. Chem. Phys.* **1990**, *93*, 1061 – 1071.
[30] S. Hammes-Schiffer, J. C. Tully, *J. Chem. Phys.* **1994**, *101*, 4657 – 4667.
[31] Maestro, version 7.5, Schrödinger, LLC, New York, NY, **2005**.
[32] W. L. Jorgensen, J. Chandrasekhar, J. D. Madura, R. W. Impey, M. L. Klein, *J. Chem. Phys.* **1982**, *79*, 926 – 935.
[33] SYBYL 8.0, Tripos International, 1699 South Hanley Rd., St. Louis, Missouri, 63144, USA.
[34] P. Sherwood, A. H. de Vries, M. F. Guest, G. Schreckenbach, C. R. A. Catlow, S. A. French, A. A. Sokol, S. T. Bromley, W. Thiel, A. J. Turner, S. Billeter, F. Terstegen, S. Thiel, J. Kendrick, S. C. Rogers, J. Casci, M. Watson, F. King, E. Karlsen, M. Sjøvoll, A. Fahmi, A. Schäfer, C. Lennartz, *J. Mol. Struct. (Theochem)* **2003**, *632*, 1.
[35] http://www.chemshell.org.
[36] E. Fabiano, Z. Lan, Y. Lu, W. Thiel in *Conical Intersections: Theory, Computation and Experiment* (*Adv. Ser. Phys. Chem. Vol. 17*) (Eds.: H. Köppel, W. Domcke, D. R. Yarkony), World Scientific, Singapore, **2011**, in press.
[37] W. Weber, PhD thesis, Universität Zürich (Switzerland), **1996**.
[38] W. Weber, W. Thiel, *Theor. Chem. Acc.* **2000**, *103*, 495 – 506.
[39] A. Koslowski, M. E. Beck, W. Thiel, *J. Comput. Chem.* **2003**, *24*, 714 – 726.
[40] M. R. Silva-Junior, W. Thiel, *J. Chem. Theory Comput.* **2010**, *6*, 1546 – 1564.
[41] E. Fabiano, W. Thiel, *J. Phys. Chem. A* **2008**, *112*, 6859 – 6863.
[42] Z. Lan, Y. Lu, E. Fabiano, W. Thiel, *ChemPhysChem*, DOI: 10.1002/cphc.20101054.
[43] W. Smith (Guest Editor), *Molecular Simulation*, **2006**, *32*, 933 – 1121.
[44] a) A. D. MacKerell, N. K. Banavali, *J. Comput. Chem.* **2000**, *21*, 105 – 120; b) N. Foloppe, A. D. MacKerell, *J. Comput. Chem.* **2000**, *21*, 86 – 104.
[45] D. Markovitsi, T. Gustavsson, A. Banyasz, *Mutat. Res. Rev.* **2010**, 704, 21 – 28.
[46] A. Abo-Riziq, L. Grace, E. Nir, M. Kabelac, P. Hobza, M. S. de Vries, *Proc. Natl. Acad. Sci. USA* **2005**, *102*, 20 – 23.
[47] A. L. Sobolewski, W. Domcke, C. Hättig, *Proc. Natl. Acad. Sci. USA* **2005**, *102*, 17903 – 17906.
[48] P. R. L. Markwick, N. L. Doltsinis, *J. Chem. Phys.* **2007**, *126*, 175102.
[49] N. K. Schwalb, F. Temps, *J. Am. Chem. Soc.* **2007**, *129*, 9272 – 9273.
[50] Z. Lan, E. Fabiano, W. Thiel, *J. Phys. Chem. B* **2009**, *113*, 3548 – 3555.
[51] Z. Lan, E. Fabiano, W. Thiel, *ChemPhysChem* **2009**, *10*, 1225 – 1229.
[52] D. Markovitsi, F. Talbot, T. Gustavsson, D. Onidas, E. Lazzarotto, S. Marguet, *Nature* **2006**, *441*, E7.
[53] F. Santoro, V. Barone, R. Improta, *Proc. Natl. Acad. Sci. USA* **2007**, *104*, 9931 – 9936.
[54] F. Santoro, V. Barone, R. Improta, *J. Am. Chem. Soc.* **2009**, *131*, 15232 – 15245.
[55] S. Perun, A. L. Sobolewski, W. Domcke, *J. Am. Chem. Soc.* **2005**, *127*, 6257 – 6265.
[56] L. Serrano-Andrés, M. Merchán, A. C. Borin, *Chem. Eur. J.* **2006**, *12*, 6559 – 6571.
[57] S. Yamazaki, S. Kato, *J. Am. Chem. Soc.* **2007**, *129*, 2901 – 2909.
[58] M. Barbatti, H. Lischka, *J. Am. Chem. Soc.* **2008**, *130*, 6831 – 6839.
[59] D. Cremer, J. A. Pople, *J. Am. Chem. Soc.* **1975**, *97*, 1354 – 1358.
[60] J. C. A. Boeyens, *J. Chem. Crystallogr.* **1978**, *8*, 317 – 320.
[61] J. D. Watson, F. H. C. Crick, *Nature* **1953**, *171*, 964 – 967.
[62] W. H. I. Hassan, W. C. Chung, N. Shimakura, S. Koseki, H. Kono, Y. Fujimura, *Phys. Chem. Chem. Phys.* **2010**, *12*, 5317 – 5328.
[63] L. Blancafort, *J. Am. Chem. Soc.* **2006**, *128*, 210 – 219.
[64] I. Conti, M. Garavelli, G. Orlandi, *J. Am. Chem. Soc.* **2009**, *131*, 16108 – 16118.
[65] D. Nachtigallová, T. Zelený, M. Ruckenbauer, T. Müller, M. Barbatti, P. Hobza, H. Lischka, *J. Am. Chem. Soc.* **2010**, *132*, 8261 – 8263.
[66] W. Humphrey, A. Dalke, K. Schulten, *J. Mol. Graph.* **1996**, *14*, 33 – 38.


  